ONERA

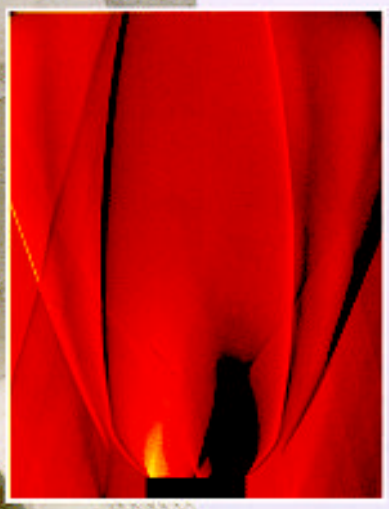

Tiré à Part

Sound generated by high speed rectangular jet using large eddy simulation

C. Seror, P. Sagaut, C. Bailly, D. Juvé**

7th International Congress on Sound and Vibration
Garmisch-Partenkirchen (Germany), July 04-07, 2000

TP 2000-145

Sound generated by high speed rectangular jet using large eddy simulation

Bruit rayonné par un jet supersonique rectangulaire

par

C. Seror, P. Sagaut, C. Bailly, D. Juvé**

* ECL-LMFA, BP 163, F-69131 Ecully Cedex

7th International Congress on Sound and Vibration
Garmisch-Partenkirchen (Germany), July 04-07, 2000

Résumé : La plupart des applications aéroacoustiques sont basées sur des méthodes hybrides permettant de calculer le bruit rayonné (analogie de Lighthill, intégrale de Kirchhoff ou équations d'Euler linéarisées) à partir du champ aérodynamique instationnaire. La simulation des grandes échelles offre un compromis intéressant entre la simulation directe et la résolution des équations de Navier-Stokes moyennées. Le présent travail porte sur l'utilisation de l'analogie de Lighthill pour le calcul de bruit de jet supersonique dont les résultats expérimentaux sont tirés des travaux de thèse de Kinzie. Une simulation des grandes échelles compressible est réalisée sur un maillage cartésien. Le mode d'instabilité associé au battement du jet est excité en sortie de buse selon la procédure de Kinzie et le champ acoustique lointain est calculé par l'analogie de Lighthill. Le champ aérodynamique calculé est en bon accord avec les résultats expérimentaux. Les résultats concernant la solution acoustique montrent une surestimation du bruit dans les basses fréquences. Les plus hautes fréquences, et notamment le screech, sont bien retrouvées.

NB : Ce document comporte 7 pages

Ce Tiré à part fait référence au Document d'Accompagnement de Publication DSNA0019

SOUND GENERATED BY HIGH SPEED RECTANGULAR JET USING LARGE-EDDY SIMULATION

Christelle Seror † , Pierre Sagaut † , Christophe Bailly ‡, Daniel Juvé ‡

† ONERA
BP72
92322 CHÂTILLON Cedex
FRANCE

‡ ECL-LMFA
BP 163
69131 ECULLY Cedex
FRANCE

seror@onera.fr

Abstract

Most of Computational Aeroacoustics applications rely on hybrid methods providing the radiated sound (using Lighthill's analogy, Kirchhoff's integral or linearized Euler's equations) from unsteady Computational Fluid Dynamics. Large-Eddy Simulation offers an interesting compromise between Direct Simulation and unsteady Reynolds Average Navier Stokes resolution. The present work is focused on Lighthill's analogy to predict noise generated by a supersonic rectangular jet based on the Kinzie experiment. A compressible Large-Eddy Simulation is performed on a cartesian mesh. The flapping mode has been excited at the nozzle exit following Kinzie's procedure and the far field noise is computed using the Lighthill analogy. The computed aerodynamic quantities agree with the experimental results. The far field noise spectra computed from the Lighthill analogy leads to an over estimation of the sound level for the lowest frequencies. Nevertheless, the amplitude and screech tone are recovered elsewhere.

INTRODUCTION

Jet noise reduction has been a topic of interest in the last years. Many methods have been investigated to reduce the noise radiated from jet. One of the most promising method is the use of jets with non circular exit geometries. Seiner *et al* [1] have shown in their experiments that noncircular geometries are able to provide a noise reduction. Indeed, the use of these geometries leads to a faster deceleration of the flow compared to that of a circular jet without lost of the aerodynamic requirement. Since the noise intensity scales exponentially with velocity, such geometries offers an interesting compromise. Kinzie [2] performed experiments with rectangular, elliptic and circular Mach 1.5 jets and investigated the aeroacoustics properties of each one. This work led to an experimental data base of acoustic and flow fluctuation measurements which offers an important issue to develop numerical tools.

Currently there are three jet noise strategies : Direct Numerical Simulation (DNS), acoustic analogy and instability wave methods.
The DNS approach is an expensive method to solve high Reynolds number turbulent flow. Indeed this approach becomes attractive in the context of computational aeroacoustics problems. Since the large coherent scales are responsible for supersonic jet noise, the resolution of all scales is not necessarily required to compute the acoustic far field. The Large Eddy Simulation has been used by many authors to reduce the number of grid points. The effects of the small scales are taken into account through a subgrid-scale turbulent model. Eddy viscosity models are often used to account the energy transfer between the large and the subgrid scales. The resolution of Euler equations using an upwind scheme for convection constitutes an other class of model. This approach, referred to as MILES (Monotone Integrated Large Eddy Simulation) by Boris *et al.* [3] ensures that the numerical dissipation recovers the energy transfer between the large scales and the subgrid ones. Nevertheless this assumption is used in the context of shear flow simulations which do not require a good approximation of the subgrid tensor.
A numerical investigation of rectangular jet noise has been performed by Chyczewski *et al.* [4, 5] using the MILES approach.
Their simulations were based on the experimental data of Kinzie [2] concerning the cold rectangular jet ($M_j = 1.56$ and $Re = 27000$). The aspect ratio AR, the equivalent diameter D_{eq}, the temperature T, the flow velocity u and sound velocity c are described in Table 1

AR	D_{eq} (cm)	M_j	T_j/T_{ext}	u_j^* mps	c_j^* mps	c_{ext}^* mps	Re
$3:1$	1.38	1.56	0.67	435	280	340	27000

Table 1: Experimental conditions. the subscript j indicates the jet values. The subscript ext denotes the ambient medium

NUMERICAL SIMULATION

Computational Domain

The computational domain used is such that $Lx = 32D_{eq}$, $Ly = 12D_{eq}$ and $Lz = 16D_{eq}$. The axis x y and z denote respectively the axial direction, the minor axis and the major axis. The mesh has 145 x 101 x 151 points in each directions x, y and z. In order to capture the shear stresses, the mesh has been stretched at the nozzle lips such that the shear layer contains approximately 10 points. In the axial direction a mesh stretching has also been applied to avoid large ratio between the three directions of the stencil.

Governing equations

The Euler equations are written in the conservative form. For cartesian coordinates, the system is given by :

$$\frac{\partial \mathbf{U}}{\partial t} + \frac{\partial \mathbf{F}}{\partial x} + \frac{\partial \mathbf{G}}{\partial y} + \frac{\partial \mathbf{H}}{\partial z} = 0 \qquad (1)$$

The convective fluxes F, G et H are given by :

$$\mathbf{U} = \begin{pmatrix} \rho \\ \rho\ u \\ \rho\ v \\ \rho\ w \\ E \end{pmatrix} \quad \mathbf{F} = \begin{pmatrix} \rho\ u \\ \rho\ u\ u + p \\ \rho\ u\ v \\ \rho\ u\ w \\ E\ u + p\ u \end{pmatrix} \quad \mathbf{G} = \begin{pmatrix} \rho\ v \\ \rho\ v\ u \\ \rho\ v\ v + p \\ \rho\ v\ w \\ E\ v + p\ v \end{pmatrix} \quad \mathbf{H} = \begin{pmatrix} \rho\ w \\ \rho\ w\ u \\ \rho\ w\ v \\ \rho\ w\ w + p \\ E\ w + p\ w \end{pmatrix}$$

The quantities ρ,u,v,w,E denote respectively the density, the axial velocity, the minor axis velocity, the major axis velocity and the total energy. The state equation for perfect gas completes the system :

$$E = \frac{p}{\gamma - 1} + \frac{1}{2}\rho(u^2 + v^2 + w^2)$$

where γ is the specific heat ratio and p is the pressure.
The spatial discretization is performed by WENO scheme [6]. The solution is advanced in time by a 3-order Rung-Kutta scheme [7]

Initial and Boundary Conditions

The jet is defined by a hyperbolic tangent velocity profile.
The jet is supposed perfectly expanded then the initial pressure in the whole domain is given by $p = T_j\rho_j/\gamma M_j^2$ The temperature profile is calculated from the Crocco-Buseman profile and the density is then deduced from the state equation for perfect gas. The unsteady nozzle conditions are obtained by exciting the flapping mode.
The excitation of the different modes (flapping and varicose) at the nozzle exit has been investigated by Chyczewski [4]. The authors compared their results to the experimental data. The flapping mode excitation results matched the experimental results while the varicose mode excitation led to a potential core greater than those obtained form the experimental data. The description of parameters of this flapping excitation is given in the reference [4].
The non reflecting boundary conditions proposed by Thompson [8, 9] have been implemented to minimize numerical reflections at far field boundaries. Further more, in order to dissipate vortices, a sponge zone described first by Berenger [10] has been added between the positions $x = 29D_{eq}$ and the downstream exit plane.

Lighthill's analogy

The acoustic field has been computed using the Lighthill analogy [11, 12]. This analogy is deduced from Navier-Stokes equation and is written as :

$$\frac{\partial^2\rho'}{\partial t^2} - c_{ext}^2\Delta\rho' = \frac{\partial^2 T_{ij}}{\partial x_i \partial x_j} \tag{2}$$

where $T_{ij} = (\rho u_i u_j + (p' - c_{ext}^2\rho')\delta_{ij} - \sigma_{ij})$ denotes the Lighthill tensor. For high Reynolds number turbulent flow, the viscous term is neglected and the Lighthill tensor reduced to $T_{ij} = (\rho u_i u_j + (p' - c_{ext}^2\rho'))$.

The radiated pressure is obtained using the 3-D free space Green function and is written in Fourier space :

$$p'(\mathbf{x},\omega) = (-\omega^2)\frac{1}{4\pi}\frac{1}{c_{ext}^2}\int_V \frac{r_i r_j}{r^3} T_{ij}(\mathbf{y},\omega) e^{-i\omega r/c_{ext}}\ d^3y \tag{3}$$

where $r = |\mathbf{x}-\mathbf{y}|$ is the distance between the observer point denoted by $\mathbf{x}$ and the current source point denoted by $\mathbf{y}$. $T_{ij}(\mathbf{y},\omega)$ is the Fourier transform in time of the Lighthill tensor. The integration is performed over a volume V which contains all acoustic sources.

NUMERICAL RESULTS

Time-averaged quantities have been computed. The centerline Mach number and velocity are respectively plotted in Figure 1 **(a)** and Figure 1 **(b)** In order to match the experimental

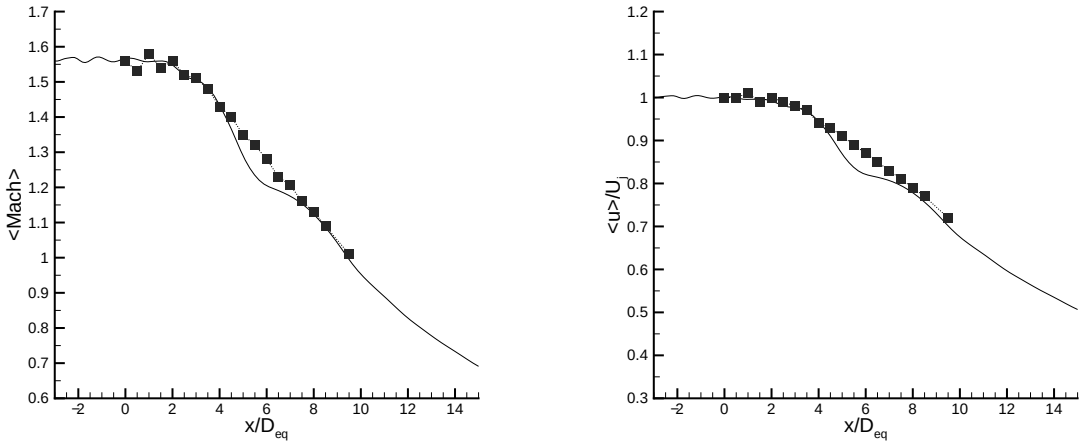

(a) **(b)**

Figure 1: **(a)** : Centerline time average Mach number - **(b)** : Centerline time average velocity ■ Experimental data ; — numerical results

data, the numerical results are shifted $-3D_{eq}$. The shift is applied so that the decay rates of the centerline mach number and velocity can be compared to the experimental data. At the end of the potential core the centerline velocity (or mach number) decays more rapidly than the experimental data. This result has also been observed by Chyczewski *et al.* [5] for all positions up to the potential core. In the present simulation, the numerical results match the experimental data up to $x = 7D_{eq}$. This decay rate indicates a strong effect of the numerical dissipation on the solution in this region. An oscillation of the centerline velocity is also observed in the core region. These oscillations were present in the experimental data and were also found by Chyczewski *et al.* [5]. This is due to a weak shock cell structure. The wave length of this oscillations has been measured and is equal to $\lambda = 1.2D_{eq}$. The model developed by Tam [13] allows the calculation of this wave length. Using this model, the wave length is $\lambda = 1.16D_{eq}$ indicating that the present simulation leads to reliable results for the representation of the shock cell structure. Acoustical results

have been obtained using the Lighthill equation described above. The volume containing the acoustic sources has been extracted from the computational domain and is defined as $V = \{x/D_{eq} \in [2,16], y/D_{eq} \in [-2,2], z/D_{eq} \in [-2,2]\}$. The far field microphone spectra from the jet are plotted on Figure 2. The microphone has been placed at the distance $R = 25D_{eq}$ in the major and minor axis planes and the angle between jet axis and the microphone is 25^o. At this position, the radiated noise is maximum according to the experimental results.

The screech tones found by Kinzie are recovered. The far field noise spectra show that

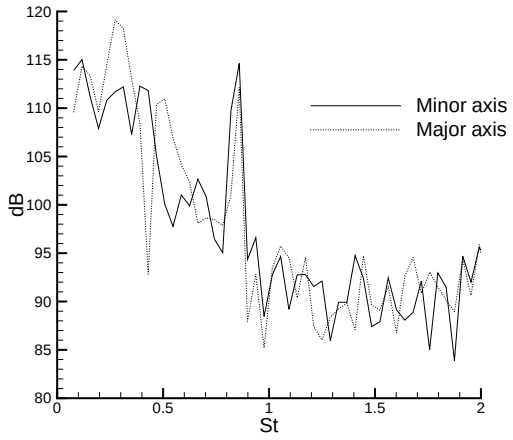

Figure 2: Far field microphone spectra. $R/D_{eq} = 25$, $\beta = 25^o$

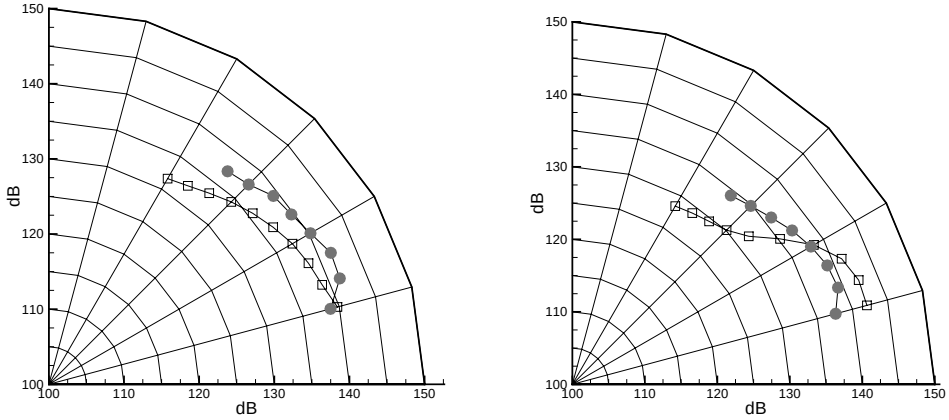

Figure 3: SPL directivity arc **(a)** : Minor axis **(b)** : Major axis
• Experimental data ; □ numerical results

the low frequency radiated noise is high in comparison with experimental results [2]. Indeed Kinzie found sound spectral level lower than $100dB$ for Strouhal number less than 0.6. For the present simulation the experimental levels are recovered for higher frequency than

$St = 0.6$. This is probably due to the forcing term. The total radiated acoustic power has been investigated for several value of β between 15^o and 60^o and has been plotted in Figure 3 **(a)** (minor axis) and **(b)** (major axis). The amplitude of the acoustic power is well estimated. Better results are obtained in the minor axis plane.

CONCLUSIONS

The MILES approach and the Lighthill analogy allow the computation of the supersonic rectangular radiated jet noise. The comparisons between experiments and simulation concerning the mean flow are reliable. The acoustical results computed from Lighthill equation show the low frequency far field spectra is over estimated. Further work concerning the influence of the excitation will be performed.

References

[1] J.M. Seiner and M.K. Ponton. Supersonic acoustic source mechanism for free jets of various geometries. In *AGARD 78thB Specialists Meeting on Combat Aircraft Noise*, (1991).

[2] K.W. Kinzie. *Aeroacoustic properties of moderate Reynolds number elliptic and rectangular supersonic jets*. PhD thesis, The Pennsylvania State University, 1995.

[3] J.P. Boris, F.F. Grinstein, E.S. Oran, and R.L. Kolbe. New insights into large eddy simulation. *Fluid Dyn. Res.*, **10**(199), (1992).

[4] T.S. Chyczewski and L.N. Long. Numerical Prediction of the Noise Produced by a Perfectly Expanded Rectangular Jet. In *AIAA Paper 96-1730*, (1996).

[5] T.S. Chyczewski, L.N. Long, and P.J. Morris. Numerical Study of Nozzle Exit Condition Effect on Jet Developpment. *AIAA Journal*, **36**(6):986–992, (1996).

[6] X.D. Liu, S. Osher, and T. Chan. Weighted Essentially Non-oscillatory Schemes. *J. Comp. Physics*, **115**:200–212, (1994).

[7] C.W. Shu and S. Osher. Efficient implementation of Essentially Non-oscillatory shock-capturing schemes. *J. Comp. Physics*, **77**:439–471, (1988).

[8] K.W. Thompson. Time dependent boundary conditions for hyperbolic system i. *J. Comp. Physics*, **68**:1–24, (1987).

[9] K.W. Thompson. Time dependent boundary conditions for hyperbolic system ii. *J. Comp. Physics*, **89**:439–461, (1987).

[10] J.P. Berenger. A perfectly matched layer for the absorption of electromagnetic waves. *J. Comp. Physics*, **114**:185–200, (1994).

[11] M.J. Lighthill. On sound generated aerodynamically. Part i : General theory. *Proc. of the Royal Society of London*, A**211**:564–587, (1952).

[12] M.J. Lighthill. On sound generated aerodynamically. Part ii : Turbulence as a source of sound. *Proc. of the Royal Society of London*, A**222**:1–32, (1954).

[13] C.K.W. Tam. On the Screech Tones of Supersonic Rectangular Jets. In *AIAA Paper 86-1866*, (1986).